J Appl Physiol 102: 417–425, 2007.
First published August 3, 2006; doi:10.1152/japplphysiol.00533.2006.

A simple technique to characterize proximal and peripheral nitric oxide exchange using constant flow exhalations and an axial diffusion model

Peter Condorelli,[1] Hye-Won Shin,[1] Anna S. Aledia,[1,3] Philip E. Silkoff,[4] and Steven C. George[1,2]

[1]*Department of Biomedical Engineering,* [2]*Department of Chemical Engineering and Materials Science,* [3]*Department of Medicine, Division of Pulmonary and Critical Care, University of California, Irvine, Irvine, California; and* [4]*Drexel University, Philadelphia, Pennsylvania*

Submitted 11 May 2006; accepted in final form 26 July 2006

Condorelli P, Shin H-W, Aledia AS, Silkoff PE, George SC. A simple technique to characterize proximal and peripheral nitric oxide exchange using constant flow exhalations and an axial diffusion model. *J Appl Physiol* 102: 417–425, 2007. First published August 3, 2006; doi:10.1152/japplphysiol.00533.2006.—The most common technique employed to describe pulmonary gas exchange of nitric oxide (NO) combines multiple constant flow exhalations with a two-compartment model (2CM) that neglects *1*) the trumpet shape (increasing surface area per unit volume) of the airway tree and *2*) gas phase axial diffusion of NO. However, recent evidence suggests that these features of the lungs are important determinants of NO exchange. The goal of this study is to present an algorithm that characterizes NO exchange using multiple constant flow exhalations and a model that considers the trumpet shape of the airway tree and axial diffusion (model TMAD). Solution of the diffusion equation for the TMAD for exhalation flows >100 ml/s can be reduced to the same linear relationship between the NO elimination rate and the flow; however, the interpretation of the slope and the intercept depend on the model. We tested the TMAD in healthy subjects ($n = 8$) using commonly used and easily performed exhalation flows (100, 150, 200, and 250 ml/s). Compared with the 2CM, estimates (mean ± SD) from the TMAD for the maximum airway flux are statistically higher ($J'aw_{NO} = 770 \pm 470$ compared with 440 ± 270 pl/s), whereas estimates for the steady-state alveolar concentration are statistically lower ($CA_{NO} = 0.66 \pm 0.98$ compared with 1.2 ± 0.80 parts/billion). Furthermore, CA_{NO} from the TMAD is not different from zero. We conclude that proximal (airways) NO production is larger than previously predicted with the 2CM and that peripheral (respiratory bronchioles and alveoli) NO is near zero in healthy subjects.

model; airway; alveolar

NITRIC OXIDE (NO) was first detected in the exhaled breath of healthy and asthmatic humans in the 1990s (1, 11). Because NO modulates many functions in the lungs (e.g., smooth muscle tone, neurotransmission, and inflammation), there has been considerable interest in understanding NO as a potentially useful noninvasive biological marker (3, 4, 7, 19, 31). Early work established a strong inverse relationship between the concentration and the exhalation flow (15, 29, 35), yet a positive relationship between the elimination rate (product of concentration and flow) and exhalation flow (29, 35). To explain these observations, two-compartment models (2CMs) were developed in which both the airways (rigid tubes) and the alveolar (flexible balloon) regions were sources of exhaled NO (13, 18, 30, 32). The 2CM was attractive because the analytical solution could easily be adapted to create algorithms that analyzed breathing maneuvers with mathematical techniques in which exhaled NO could be partitioned into alveolar (peripheral) and airway (proximal) contributions. This led to the rapid application of these techniques to characterize proximal and peripheral NO in a range of normal and pathological conditions including exercise (25), asthma (8, 14, 16, 17, 26, 30), chronic obstructive pulmonary disease (14), cystic fibrosis (28), and scleroderma (10).

The simplicity of the 2CM is both its strength and weakness. Although the initial description of the model (32) considered the increasing cross-sectional area with distance into the airway tree (i.e., the "trumpet" shape), the subsequent early descriptions neglected this feature (13, 18, 30), and all of the early models neglected axial (as opposed to radial) diffusion of NO in the gas phase. More recently, advanced theoretical and experimental studies (with heliox) by our group (21–24) and others (36) have now established that both the trumpet geometry and gas-phase axial diffusion of NO are critical features of NO exchange that should be considered in the analytical methods.

Although several techniques have been presented that employ a breathhold (single or multiple; Refs. 22, 33) or tidal breathing (6) maneuver, the most common method by far is a series of single exhalation maneuvers from maximal inspiration in which the exhalation flow is held constant during a single exhalation, but different exhalation flows are used (i.e., multiple constant flow exhalations; Ref. 9). In addition, the constant flow exhalation is the recommended maneuver of both the American Thoracic Society (ATS) and the European Respiratory Society (2), usually performed at a single exhalation flow. Although our most recent work has incorporated axial diffusion and the trumpet shape of the airway tree into the governing material balance equations of the 2CM, the solutions have required cumbersome numerical techniques or considered a transient no-flow (breathhold) condition (21–24), which may be difficult for some patients. The goals of the current study are threefold: *1*) develop a steady-state model of NO exchange that considers axial diffusion and the trumpet shape of the airway tree, *2*) use the model to develop an algorithm that analyzes a series of steady-state constant flow exhalations and partitions exhaled NO into proximal and peripheral components, and *3*) compare the performance of the new model with the earlier simpler model that neglects axial diffusion and the trumpet shape of the airway tree.

Address for reprint requests and other correspondence: S. C. George, Dept. of Biomedical Engineering, 3120 Natural Sciences II, Univ. of California, Irvine, Irvine, CA 92697-2715 (e-mail: scgeorge@uci.edu).

The costs of publication of this article were defrayed in part by the payment of page charges. The article must therefore be hereby marked "*advertisement*" in accordance with 18 U.S.C. Section 1734 solely to indicate this fact.

METHODS

Experimental exhaled NO. We collected exhaled NO concentration and exhalation flow from healthy nonsmoking, nonasthmatic adults with no history of respiratory disease. The protocol focused on an exhalation flow range that is practical and easy to perform in terms of the magnitude of the flow itself, as well as the number of flows and breathing maneuvers. In addition, we sought high enough flows to ensure that the wall flux of NO from the airway tree (Jaw_{NO}, pl/s) is constant (independent of flow) and approaches the maximum airway wall flux of NO ($J'aw_{NO}$, pl/s; Ref. 9). This condition is safely met for flows >100 ml/s in healthy adults (9, 32) and greatly simplifies the solution of the governing equation (see *Model* and APPENDIX). Thus the target flows were 100, 150, 200, and 250 ml/s. These flows have been commonly employed by other research groups, and can be performed by nearly all subjects. Furthermore, by performing each maneuver in triplicate, we limited the number of exhalation flows to 12 for each subject. The group consisted of eight subjects (5 female) with (mean ± SD) age, height, weight, and forced expiratory volume in 1 s (FEV_1) (Vmax229; Sensormedics, Yorba Linda, CA) of 31 ± 5 yr, 165 ± 10.1 cm, 62.3 ± 12.3 kg, and 3.5 ± 0.6 liters (102 ± 4.5% predicted), respectively (see Table 1 for details). Each exhalation flow was achieved using flow restrictors. Flow, pressure, and NO concentration (model 280B, Ionics, Boulder, CO) for each maneuver were recorded simultaneously. The protocol was approved by the Institutional Review Board at the University of California, Irvine, and written informed consent was obtained from each subject.

We previously demonstrated that the slope of the exhalation NO profile in phase III is statistically negative (between 4 and 12% of the concentration per liter exhaled) at a constant exhalation flow (35). Thus, when determining exhaled NO concentration ($C_{E_{NO}}$) for multiple exhalation flows, it is important to analyze the exhaled concentration over a similar lung volume. We also wanted to ensure that the airway tree had been sufficiently emptied of the inspired air and that we considered the variation in lung volume between subjects. Thus we plotted exhaled concentration as a function of the number of airway volumes (Vaw) exhaled. Vaw was estimated as the sum of the subjects age in years and the ideal body weight in pounds (5, 22, 33). Then $C_{E_{NO}}$ was calculated as the mean concentration between five and ten exhaled airway volumes. The minimum of five airway volumes was chosen to completely washout the airway tree of the inspired air and allow a steady flow to be achieved. A maximum of ten was chosen to assure analysis over a time window (~3–7 s depending on the flow) that is similar to the recommended guidelines of the American Thoracic Society (3 s) and European Respiratory Society (2). A breathing maneuver was excluded if the standard deviation of the exhalation flow over this same exhaled volume range exceeded 5% (i.e., the maneuver was not considered "constant exhalation flow").

Model. Models for vital capacity maneuvers at constant exhalation flow assume that the concentration and flux of NO in the proximal (airway) and peripheral (alveolar) regions of the human lungs approach steady state (i.e., are independent of time), and a steady ("plateau") concentration ($C_{E_{NO}}$) is achieved in the exhaled air at the mouth. The trumpet model with axial diffusion (TMAD) characterizes airway geometry by appropriately scaling the lengths and diameters of Weibel's data (37) of the human airway tree, based on the conducting airway volume (Vaw) of the oral cavity, oropharynx, and generations 0–17 for each subject (see Table 1). Figure 1 depicts the mapping of airway dimensions to a "trumpet geometry," using the following logarithmic relationship that is consistent with our previous reports (21, 22):

$$A = A_1\left(\frac{z}{z_1}\right)^{-m} \quad (1)$$

where A is the airway cross-sectional area, z is the axial position, subscript 2 refers to the axial position at the mouth (subscript 1 refers

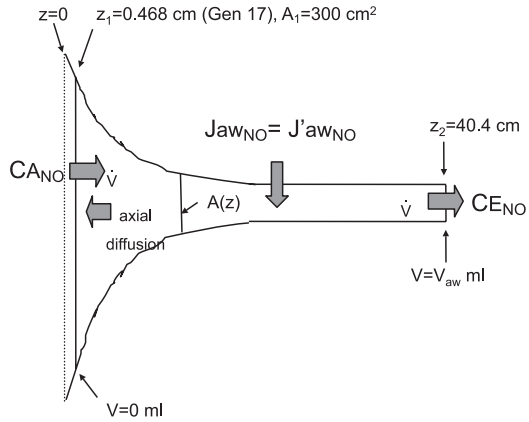

Fig. 1. Schematic of the trumpet model. Alveolar air with nitric oxide (NO) steady-state alveolar concentration ($C_{A_{NO}}$) exits the alveolar region at position z_1 (generation 17) and is transported toward the mouth (position z_2) by convection at a steady volumetric flow rate ($\dot{V}$). NO is added to the airstream at a rate equal to the wall flux of NO from the airway wall (Jaw_{NO}; pl/s). Because the flow is larger than 100 ml/s, Jaw_{NO} can be considered constant and equal to the maximum airway flux $J'aw_{NO}$ (9). Thus the concentration increases with z-position and the concentration at the mouth (the exhaled concentration, $C_{E_{NO}}$) is described by *Eq. 2*. Axial diffusion of NO is described by Fick's 1st law of diffusion and transports NO from high to low concentration; thus NO is simultaneously transported by diffusion in the axial direction back toward the alveolar region. Airway volume is defined as the volume between positions z_1 and z_2 and is estimated in ml as the sum of the subjects age in years plus ideal body weight in pounds (5, 33). The cross-sectional area of the trumpet decreases with increasing z-position and is determined by the relationship in *Eq. 1* by mapping the airway dimensions to that of the Weibel symmetric bifurcating airway tree (37).

Table 1. *Physical characteristics of subjects*

Subject	Sex	Age, yrs	Ht, cm	Wt, kg	Iwt, kg	V_{aw}, ml	FEV_1, liters, %predicted
1	F	35	150	44	50	145	2.59, 104
2	M	29	168	66	65	173	3.59, 96
3	M	31	170	73	67	179	3.62, 93
4	F	25	160	49	57	150	3.23, 106
5	M	27	178	79	73	188	4.75, 103
6	F	28	178	69	67	175	3.63, 102
7	F	30	163	53	58	158	3.17, 105
8	F	39	157	66	55	160	3.07, 107
Mean		31	165	62	62	166	3.50, 102
SD		5	10	12	8	15	0.6, 4.5

Ht, height; Wt, body weight; Iwt, ideal body weight; V_{aw}, volume of the airway compartment estimated in ml as the sum of the subjects ideal body weight (lbs) plus age (yrs Ref. 34); FEV_1: forced expiratory volumes in 1 s (liters and %predicted).

to the axial position at the end of generation 17; see Fig. 1), and $m = 2$ provides an excellent match to the data of Weibel (22, 37). The APPENDIX provides details of a solution to the steady-state diffusion equation generating the following solution for the exhaled concentration of NO at the mouth,

$$C_{E_{NO}} = C_{A_{NO}} + \frac{J'aw_{NO}}{\dot{V}} \cdot f(\dot{V}, D_{NO,air}, A_1) \quad (2)$$

where f is a function (see APPENDIX) of the exhalation flow, the molecular diffusivity of NO in the insufflating gas (i.e., $D_{NO,air}$ or axial diffusion), and the cross-sectional area of the airway tree at the airway-alveolar junction (i.e., the shape of the trumpet). The key assumption in the solution to the governing equation is that the flux of NO from the airway tree is a constant (i.e., does not depend on flow), and thus our solution is valid for approximately exhalation flows >100 ml/s in healthy adults. Note that as f approaches unity, the simple solution of the 2CM is attained (9, 32, 35).

Parameter estimation. Equation 2 can be simplified more by limiting the flow to the range to $100<\dot{V}<250$ ml/s, which is the range commonly employed in experimental studies including the current study. In this range, f is nearly a linear function of $\dot{V}$ ($r^2 = 0.98$, see APPENDIX, Fig. 5) and can be approximated by f = (0.00078 s/ml)*$\dot{V}$ + 0.57. If this relationship is inserted into *Equation 2*, and both sides of the equation are multiplied by $\dot{V}$, the following linear relationship for the elimination rate ($\dot{V}_{NO}$, pl/s) of NO as a function of flow is attained,

$$\dot{V}_{NO} = (C_{A_{NO}} + J'aw_{NO} \cdot 0.00078)\dot{V} + \frac{J'aw_{NO}}{1.7} \quad (3)$$

where the factor 1.7 is the inverse of 0.57. Thus the model predicts that a plot of $\dot{V}_{NO}$ vs. $\dot{V}$ produces a linear relationship in which the slope, S, is equal to $C_{A_{NO}} + J'aw_{NO}$*0.00078 and the intercept, I, is equal to $J'aw_{NO}/1.7$. Hence, $C_{A_{NO}}$ and $J'aw_{NO}$ can be estimated from a plot of $\dot{V}_{NO}$ vs. $\dot{V}$ using the TMAD and the following simple relationships,

$$C_{A_{NO}} = S - I\left(\frac{0.00078 \text{ s/ml}}{0.57}\right) = S - \frac{I}{740 \text{ ml/s}} \quad (4)$$

$$J'aw_{NO} = 1.7 \cdot I \quad (5)$$

where S is the slope and I is the *y*-intercept using simple linear regression. This can be contrasted with the 2CM in which $C_{A_{NO}}$ and $J'aw_{NO}$ can be approximated as simply S and I, respectively (9, 32, 35). Values for $J'aw_{NO}$ and $C_{A_{NO}}$ were thus determined by applying linear least squares to a plot of $\dot{V}_{NO}$ vs. $\dot{V}$ for each subject using both the 2CM and the TMAD (*Eqs. 4* and *5*). The slope was constrained to be greater than or equal to zero.

We previously described in a response to a letter to the editor of the *Journal of Applied Physiology* (20) the advantages of using $\dot{V}_{NO}$ vs. $\dot{V}$ instead of alternate forms that use $C_{E_{NO}}$ as the dependent variable. In brief, using $\dot{V}_{NO}$ as the dependent variable effectively places more weight on the data obtained at higher flow. This can be justified because the assumption of a constant wall flux becomes more accurate as the flow increases (and thus the model is more accurate); thus this technique provides a more accurate estimate of $J'aw_{NO}$ and $C_{A_{NO}}$.

Statistics. Confidence intervals (95%) for the determined parameters were calculated assuming a normally distributed error using the *t*-statistic for the slope and intercept of $\dot{V}_{NO}$ vs. $\dot{V}$ for each subject. Differences between the determined parameters using the TMAD and 2CM models as well as comparing the determined parameters to a mean value of zero were calculated using a paired *t*-test or single population *t*-test, respectively. Statistical significance was assumed for $P < 0.05$.

RESULTS

In each subject, one or more maneuvers were eliminated by not meeting the criteria for a constant exhalation flow. Figure 2 shows representative exhalation profiles from *subject 1* for a typical maneuver that was included (Fig. 2*A*) and excluded (Fig. 2*B*). Of the 96 breathing maneuvers (12 maneuvers/subject × 8 subjects), 65 (68%) were included for further analysis, the remaining 31 having been eliminated by exceeding the maximum variation in flow during the analysis window (standard deviation >5%). Figure 2*C* demonstrates $C_{E_{NO}}$ of the profiles that met the inclusion criteria as a function of exhalation flow for all eight subjects. The data demonstrate the inverse relationship between $C_{E_{NO}}$ and $\dot{V}$ for all eight subjects that has been previously reported (15, 29, 35).

Figure 3 demonstrates the relationship between $\dot{V}_{NO}$ and $\dot{V}$ for all eight subjects, including the best fit line. $\dot{V}_{NO}$ has been calculated using the individual NO concentrations and flows shown in Fig. 2*C*. Note that a positive relationship between $\dot{V}_{NO}$ and $\dot{V}$ exists for seven of the eight subjects. For *subject 5*, the best fit line (constraining the slope to be ≥0) has a zero slope. Figure 4 compares the estimated values for $C_{A_{NO}}$ and $J'aw_{NO}$ using the 2CM and TMAD (*Eqs. 4* and *5*) models. The mean (±SD) value of $C_{A_{NO}}$ for the TMAD model is 0.66 ± 0.98 parts/billion (ppb), which is not statistically different from zero ($P > 0.05$) and statistically smaller than the mean value determined with the 2CM model (1.2 ± 0.80 ppb, which is statistically larger than zero). The mean (±SD) value of $J'aw_{NO}$ for the TMAD model is 770 ± 470 pl/s, which is statistically larger (1.7 times, see *Eq. 4*) than the mean value determined from the 2CM model (440 ± 270 pl/s).

An important consideration in a method to determine unknown parameters is the uncertainty in the estimate. Table 2 presents the uncertainty (95% confidence interval) in the estimates for $C_{A_{NO}}$ and $J'aw_{NO}$ for each of the subjects and for each of the models. The 95% confidence interval for $C_{A_{NO}}$ spans zero for six and seven subjects, respectively, for the 2CM and TMAD models. For $J'aw_{NO}$, the 95% confidence interval spans zero for only three of the eight subjects for both models. The mean maximum deviation from the central value for $J'aw_{NO}$ (for both models) is 154 ± 225%; however, this value is significantly skewed by *subject 8,* in whom the central value is small (94 pl/s) and the uncertainty high. If this subject is removed, the mean maximum deviation is 74 ± 41%.

DISCUSSION

We have described a new technique to partition proximal and peripheral NO exchange in the lungs that incorporates previously neglected, yet relevant, physical features of the airway tree and gas exchange while maintaining mathematical and computational simplicity. By limiting the flow range to 100–250 ml/s, we are able to incorporate both the trumpet shape of the airway tree and axial diffusion of NO yet still produce a solution of the governing equation and computational technique that uses the slope and intercept of NO elimination vs. flow. The result is a 1.7-fold larger flux of NO from the airway tree and a near zero alveolar (peripheral) NO concentration. These results are consistent with previous, yet more complicated, numerical models, which included the trumpet shape and axial diffusion (21–24, 36). Thus our technique provides a more accurate description of NO exchange dynamics than the previously described and commonly employed 2CM for constant flow exhalations, but maintains simplicity,

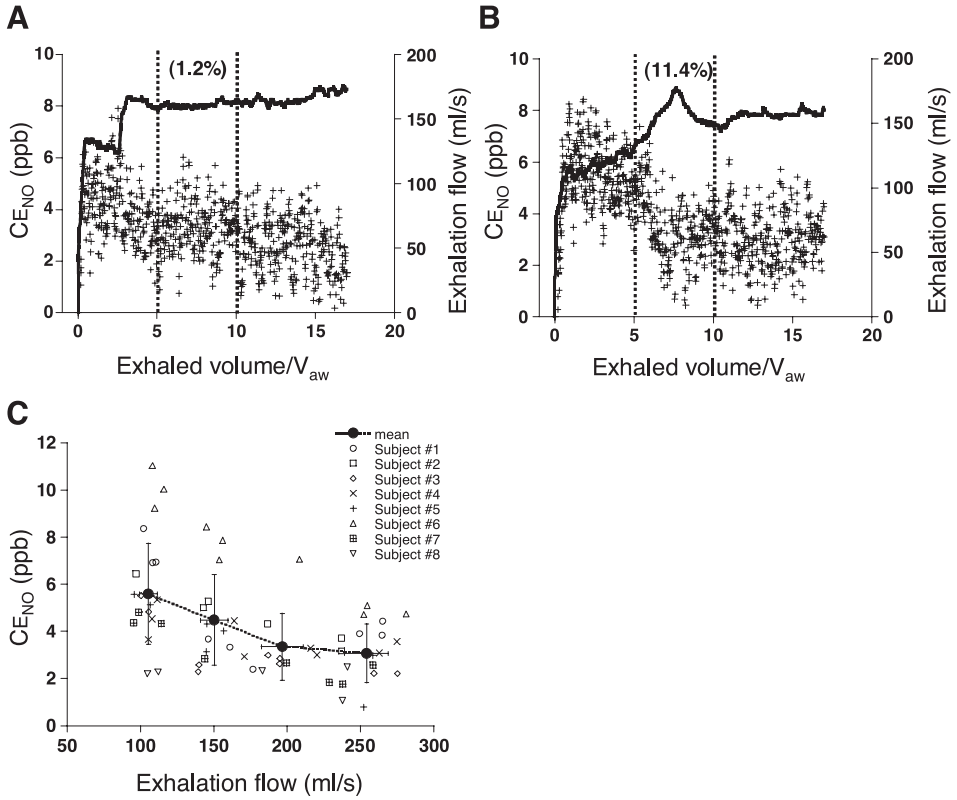

Fig. 2. Determination of plateau exhaled concentrations. Representative exhalation flow profiles from *subject 1* at the targeted exhalation flow of 150 ml/s for an exhalation maneuver included in the final analysis (*A*) and a maneuver excluded from analysis (*B*). The "+" are NO concentration from an unfiltered signal and the solid line is exhalation flow. The space between the vertical dashed lines represents the window of analysis (between 5 and 10 exhaled airway volumes). Note that in maneuver marked for inclusion, several airway volumes are needed to be exhaled before a steady flow is achieved; then, during the analysis window, the standard deviation of the flow is 1.2% (number in parenthesis). Note also that despite a constant flow, a negative slope in the NO concentration is evident highlighting the need to analyze the profiles over a constant exhaled volume window that is scaled to the subjects lung volume. In the maneuver marked for exclusion, the exhalation flow is not constant (standard deviation 11.4%) until after the analysis window. The last panel (*C*) summarizes the plateau NO concentrations from all 8 subjects of the profiles marked for inclusion, including the mean value (●) at each of the targeted exhalation flows (100, 150, 200, and 250 ml/s).

and thus may be broadly useful to describe proximal and peripheral NO exchange in lung disease.

We previously showed that adding axial diffusion of NO alone (i.e., maintaining the cylindrical geometry) does not significantly impact NO exchange (21, 22). However, the combination of axial diffusion with the trumpet shape dramatically increases the loss of NO to the alveolar region. This is due to the fact that the rate of axial diffusion is proportional to the product of the concentration gradient (change in concentration with axial position) and the cross-sectional area (see APPENDIX). The dramatic increase in the cross-sectional area in the peripheral regions of the lungs effectively reduces the resistance of NO diffusion in the axial direction, making this a significant physical force that cannot be neglected. Because the observed concentration of NO at the mouth is unchanged, the predicted flux of NO from the airway tree must increase to account for the loss of NO due to back diffusion into the alveolar region. Previous estimates by our group and others (21–24, 36) using breathhold techniques has estimated this increase to be between two- and fivefold, which is consistent with our current prediction using constant flow exhalations (1.7-fold increase).

The large pool of blood in the alveolar region provides a near infinite sink (primarily hemoglobin) to scavenge NO. Thus any additional NO that diffuses from the airway tree toward the alveolar region is immediately bound and does not impact the steady alveolar concentration. We previously demonstrated that the relative impact of axial diffusion decreases as exhalation flow increases (23). This is due to the shift in the balance between convection (movement of NO from the bulk flow of air) of NO and diffusion (Brownian motion of NO molecules) of NO. The rate of convective transport of NO increases in proportion to the exhalation flow, but does not impact the rate of axial diffusive transport. Thus, as flow increases, the loss of NO to the alveolar region by diffusion decreases. This phenomenon by itself can produce a positive slope in the plot of NO elimination vs. exhalation flow of ~1 pl/s per ml/s (ppb) over a flow range of 100–250 ml/s in healthy subjects (23). The relative impact should depend on the flux of NO from the airway tree. The larger the airway flux, the larger the gradient of NO in the airway tree, and thus the larger the impact of axial diffusion. This trend is exactly what our model predicts. The alveolar concentration is equal to the value of slope of the NO elimination vs. flow minus a term that is proportional to the airway flux (*Eq. 5*). For example, for our predicted mean airway flux of 770 pl/s, the impact of axial diffusion, and the trumpet shape of the airway tree can produce a slope of 0.60 ppb [I/740 s/ml = $J'aw_{NO}$/(1.7*740 s/ml), *Eqs. 4* and *5*], which must be subtracted from the slope to reveal the true alveolar concentration. Because the mean slope of NO elimination vs. flow in our subjects was only 1.2 ppb, the predicted alveolar concentration by the TMAD is near zero (0.66 ppb) and consistent with our previous predictions using more complex numerical solutions and breathhold techniques (21, 23, 24).

The result in Fig. 4 and Table 2 that C_{ANO} is negative using the TMAD model in two subjects should not be interpreted as a true negative concentration as this has no physical meaning. The 95% confidence interval presented in Table 2 for C_{ANO} is the true range of possible values (with 95% confidence), and this range includes positives values for all subjects. The fact that the 95% confidence interval includes negative values simply reflects the noise and error in the experimental measurement and mathematical model. It is important to note that

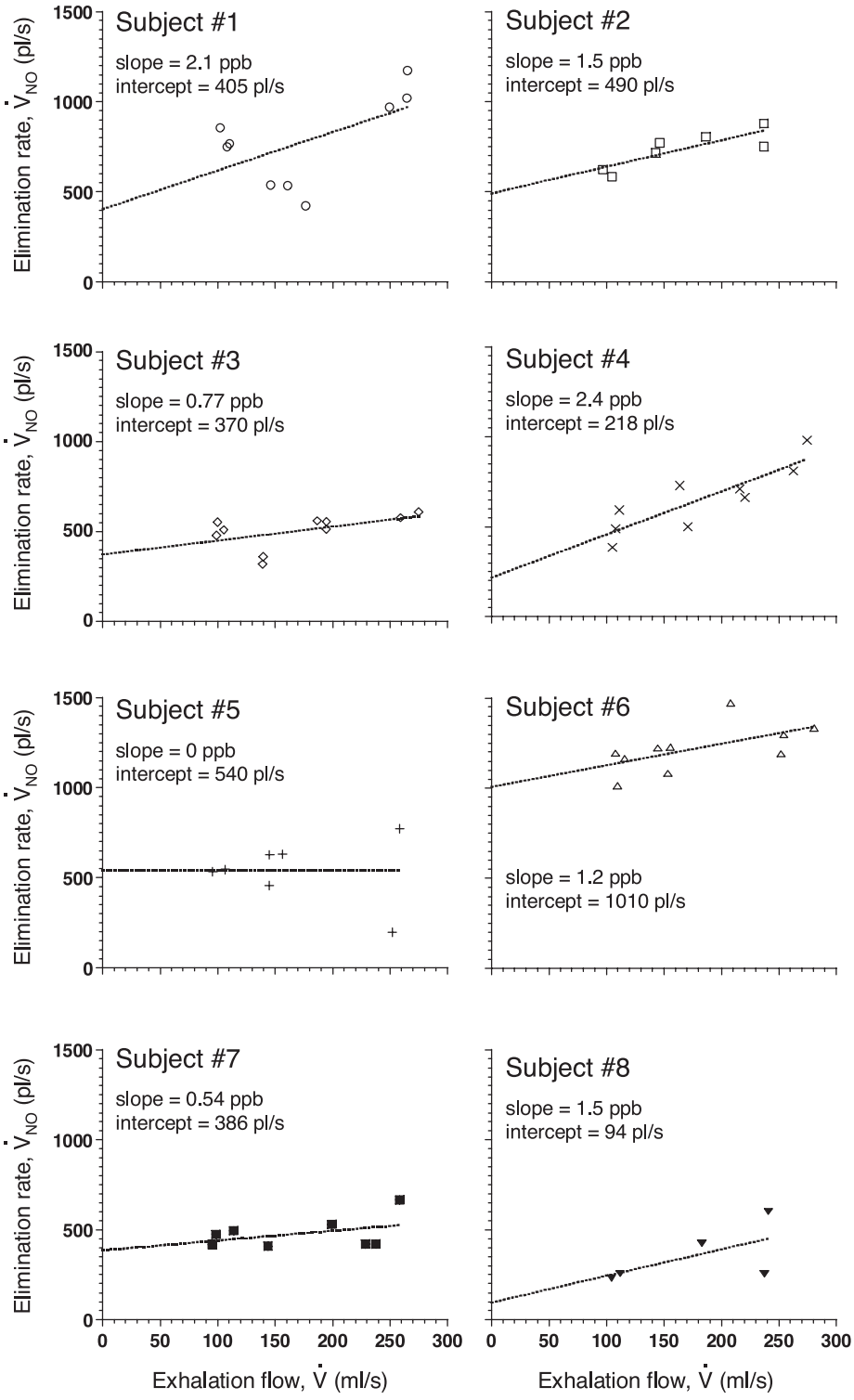

Fig. 3. NO elimination rate ($\dot{V}_{NO}$) vs. $\dot{V}$ is presented for all 8 subjects using only the exhalation profiles that met the requirements for inclusion (Fig. 2). The solid line is the best fit line using linear regression and the best fit slope and intercept for this line are also shown. The slope was greater than zero for all subjects except *subject 5* (equal to 0).

the mean value for all subjects is greater than zero, albeit not statistically different from zero.

An important limitation in the current technique is the inability to characterize the airway diffusing capacity of NO, or Daw_{NO} (9). We and others previously showed that to estimate Daw_{NO}, the exhalation flow must be low enough such that the concentration of NO in the airway tree, C_{NO}, can reach a high enough level to decrease the airway flux (9, 13, 18, 30, 33). In other words, the airway flux is no longer a constant and equal to the maximum airway flux. This phenomenon occurs for exhalation flows less than ~50 ml/s (5*Daw_{NO}) in healthy subjects (9). However, even when such low flows are used, the uncertainty in determining Daw_{NO} remains large, and obtaining a reliable plateau exhaled concentration is difficult for many subjects due to the necessary long exhalation time. For example, if one were to examine the same exhaled volume

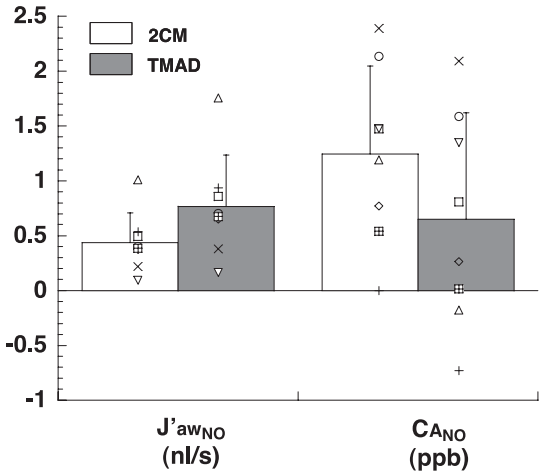

Fig. 4. Determined parameters characterizing peripheral ($C_{A_{NO}}$) and proximal ($J'aw_{NO}$) NO exchange using the two-compartment (2CM) model and the trumpet-model with axial diffusion (TMAD). The mean of the 8 subjects (bar), standard deviation of the mean (error bar), and data points (symbols) for each of the subjects are shown. CA_{NO} and $J'aw_{NO}$ were determined using the slope and intercept of $\dot{V}_{NO}$ vs. $\dot{V}$ shown in Fig. 3 and *Eqs. 4* and *5* in METHODS.

region as in the current study (between 5 and 10 exhaled airway volumes), one would need to exhale for between 30 and 60 s, assuming an exhalation flow of 25 ml/s and an airway volume of 166 ml (mean of the 8 subjects in this study). Daw_{NO} may be a useful steroid-independent parameter in asthma (26, 30), and we previously showed that a series of breathhold maneuvers may be the most accurate method to characterize its magnitude (22, 26).

We previously used the TMAD model to determine the airway NO parameters $J'aw_{NO}$ and Daw_{NO} using a series of breathhold maneuvers (21, 22). In this technique, the governing equation is unsteady and there is no convection (analysis considers only the NO accumulation during the breathhold). In these studies, the mean $J'aw_{NO}$ was 4,150–4,350 pl/s, which is 5.4–5.6 times larger than the estimate in the current study (770 pl/s). However, the impact of axial diffusion is similar predicting a 2.6-fold increase in $J'aw_{NO}$ (e.g., 4,350 pl/s compared with 1,704 pl/s in Ref. 22). Thus the difference in the techniques is primarily the magnitude of $J'aw_{NO}$. This difference may be due to different subject populations. There is significant variation in NO elimination among the healthy population and our current study included only eight subjects. In the current study, the estimated $J'aw_{NO}$ using the 2CM (440 pl/s) is smaller than most other estimates using constant flow exhalations (range 700–1,280 pl/s; Ref. 9). In addition, the difference in the magnitude of $J'aw_{NO}$ may reflect differences in the techniques. For example, the breathhold technique is a transient technique, and the estimated value of $J'aw_{NO}$ is proportional to the estimated value of Vaw. In contrast, the current technique depends on steady-state measurements of exhaled concentration and flow and is independent of Vaw (with the minor exception that the window of analysis to determine CE_{NO} is based on Vaw). In any event, although the relative impact of axial diffusion and the trumpet shape is consistent between the techniques, caution must be exercised in comparing absolute values of the determined parameters between techniques.

The uncertainty in estimating $J'aw_{NO}$ in the current technique is significant in healthy subjects. In three of the subjects, the 95% confidence interval spanned zero, suggesting not that $J'aw_{NO}$ was necessarily zero (the NO is coming from somewhere), but rather that the technique could not determine a positive value with 95% confidence. The uncertainty is due to the noise in the experimental data of plotting $\dot{V}_{NO}$ vs. $\dot{V}$ and using only 5–10 data points (depending on the subject). Additional breathing maneuvers will improve the accuracy of the estimated value at the expense of additional effort on the part of the subject. Single breath techniques with a prescribed decrease in the exhalation flow during the maneuver (26, 27, 33) may provide a more accurate estimate of airway and alveolar NO contributions with much fewer breathing maneuvers, but they require more sophisticated mathematical tools and have not yet been tested with axial diffusion and the trumpet shape of the airway tree.

Finally, the flow range used in the current study was chosen based on the relative ease at which subjects can perform them and the need to keep the airway flux constant (i.e., $J'aw_{NO} >> Daw_{NO} * C_{NO}$). However, several research groups have presented constant flow exhalations using flows larger than 250 ml/s (13, 16), and in healthy subjects the airway flux may be constant for flows as low as 50 ml/s (9). Furthermore, the

Table 2. *Airway and alveolar NO exchange parameters and confidence intervals*

	2CM						TMAD					
	CA_{NO}			$J'aw_{NO}$			CA_{NO}			$J'aw_{NO}$		
Subject	Central	Lower	Upper	Central	Lower	Upper	Central	Lower	Upper	Central	Lower	Upper
1	2.1	−0.56	4.8	410	−100	910	1.6	−1.8	4.8	710	170	1600
2	1.5	0.34	2.6	490	300	690	0.81	−0.59	2.6	860	500	1,200
3	0.77	−0.26	1.8	370	190	560	0.26	−1.0	1.8	650	330	970
4	2.4	1.1	3.7	220	−25	460	2.1	0.49	3.7	380	−40	800
5	0.00	−3.5	2.8	540	40	1,200	−0.73	−5.1	2.8	940	70	2,000
6	1.2	−0.09	2.5	1,000	770	1,200	−0.18	−1.8	2.5	1,800	1,300	2,200
7	0.54	−0.66	1.7	390	170	610	0.020	−1.5	1.5	670	290	1,000
8	1.5	−2.0	5.0	94	−560	750	1.40	−3.5	6.1	160	−980	1,300
Mean	1.2			440			0.66*,†			770†		
SD	0.80			270			0.98			470		

2CM, 2-compartment model; TMAD, trumpet model with axial diffusion; CA_{NO}, alveolar concentration of NO; $J'aw_{NO}$, maximum airway flux of NO; "lower" and "upper" refer to the limits of the 95% confidence interval for the central determined value. *Not statistically different from zero ($P > 0.05$); †statistically different from the 2CM model.

Table 3. *Approximation for f and subsequent relationships for C_{ANO} and $J'aw_{NO}$*

Flow Range, ml/s	$f \cong a * \dot{V} + b$			$C_{ANO} \cong S - I/c$	$J'aw_{NO} \cong I * d$
	a, s/ml	b	r^2	c, ml/s	d
50–250	0.00100	0.53	0.94	530	1.9
50–500	0.00056	0.59	0.89	1100	1.7
100–250	0.00078	0.57	0.98	740	1.7
100–300	0.00068	0.59	0.97	860	1.7
100–400	0.00055	0.61	0.95	1100	1.6
100–500	0.00045	0.63	0.94	1400	1.6

S, slope of $\dot{V}_{NO}$ (pl/s) vs. $\dot{V}$ (ml/s); I, intercept of $\dot{V}_{NO}$ (pl/s) vs. $\dot{V}$ (ml/s); r^2, coefficient of determination for the linear approximation of the complex function f (19 data points with evenly distributed values for exhalation flow were used in the linear regression).

applicable flow range in disease states such as asthma has not yet been determined. It appears that both the wall concentration (Caw_{NO}) and Daw_{NO} are elevated in asthma (26, 30) and thus the applicable flow range may be similar to healthy subjects (i.e., a larger Daw_{NO} requires a larger minimum flow, but a larger wall concentration increases $J'aw_{NO}$ and reduces the minimum flow). The critical feature to determine the applicability of the current model is an observed linear relationship between $\dot{V}_{NO}$ and $\dot{V}$. Nonetheless, the flow range used will impact the approximate linear relationship for f and subsequent relationships for C_{ANO} and $J'aw_{NO}$. Thus Table 3 presents the approximation for f and relationships for C_{ANO} and $J'aw_{NO}$ for several additional flow ranges that might be employed using this technique. Note that as higher flows are considered in the analysis, axial diffusion becomes less important, and the slope and intercept of $\dot{V}_{NO}$ vs. $\dot{V}$ more closely approaches C_{ANO} and $J'aw_{NO}$, respectively.

In summary, we have described a simple technique to partition airway (proximal) and alveolar (peripheral) NO using a series of constant flow exhalations. The model considers the combination of steady-state flow conditions, the trumpet shape of the airway tree (increasing cross-sectional area with distance into the lungs), and axial diffusion of NO. The technique uses the previously described and commonly employed plot of NO elimination vs. exhalation flow, but the presence of the trumpet shape and axial diffusion produces an alternate interpretation of the resulting slope and intercept. The result is a 1.7-fold increase in the predicted flux of NO from the airway tree and an alveolar concentration that is near zero. The technique includes the most relevant anatomical and physical features of the lungs (i.e., the trumpet shape of the airways and axial diffusion), yet maintains simplicity by considering only steady-state flows that are readily performed by most adult subjects. Thus the technique may be useful to a broad range of investigators in characterizing proximal and peripheral NO in lung pathology.

APPENDIX

Model development. The development of the governing equation for the model begins with a differential mass balance over a thickness Δz in the airway tube. The salient features of the model are *1*) a cross-sectional area, A, that depends on z-position (trumpet shape, *Eq. 1*); *2*) a constant airway flux per unit volume from the airway wall (radial diffusion) equal to the total maximum airway wall flux from the entire airway tree, $J'aw_{NO}$ (pl/s) divided by the airway volume, Vaw; *3*) axial diffusion (in the z-direction) of NO in the gas phase is governing by Fick's 1st law of diffusion ($A*D_{NO,air}*dC_{NO}/dz$, pl NO/s), where $D_{NO,air}$ is the molecular diffusivity of NO in air; *4*) convection of NO in the z-direction is characterized by the bulk exhalation flow, $\dot{V}$ (ml/s); and *5*) steady-state conditions. The result is the following form of the convective-diffusion equation describing the concentration of NO and C_{NO} (ppb or pl NO/cm^3) in the airway tree as a function of position,

$$\frac{d^2C_{NO}}{dz^2} + \left[\frac{1}{A}\frac{dA}{dz} - \frac{\dot{V}}{D_{NO,air}A_{cs}}\right]\frac{dC_{NO}}{dz} + \frac{J'aw_{NO}}{D_{NO,air}V_{aw}} = 0 \qquad (A1)$$

with the following two boundary conditions,

$$C_{NO}(z = z_1) = C_{ANO} \qquad (A2)$$

$$\frac{dC_{NO}}{dz}(z = z_2) = 0 \qquad (A3)$$

The first boundary condition (*Eq. A2*) simply states that the concentration of NO entering the trumpet at position z_1 (generation 17) is equal to the alveolar concentration, C_{ANO}. The second boundary condition states that convective flow is large enough near mouth (position z_2) that the concentration gradient in the z-position is negligible or approaches zero (21–24).

The values for z_1 and z_2 are determined using the data from Weibel (37) for generations 0–23 and from Hanna and Scherer (12) for the dimensions of the oropharynx and oral cavities. Thus z_1 = 0.468 cm (end of generation 17) and z_2 = 40.4 cm. Note then that the airway volume can be easily estimated by integrating Adz over the length of the trumpet,

$$V_{aw} = \int_{z_1}^{z_2} A(z)dz = A_1 z_1 \int_1^{x_2} x^{-2}dx = A_1 z_1(1 - x_2^{-1}) \qquad (A4)$$

where $x = z/z_1$ (and thus $x_2 = z_2/z_1$ = 84.6) and A_1 is the cross-sectional area at position z_1 (300 cm^2, Fig. 1). *Equation A4* produces a value for Vaw of 142 ml that is in close agreement with our population mean estimate of 166 ml using the sum of the subject's ideal body weight in pounds plus age in years.

The solution to the governing equation (*Eq. A1*) is most readily attained by defining the following nondimensional parameters: $\phi = C_{NO}/C_{ANO}$, $x = z/z_1$, $Pe_1 = z_1\dot{V},D_{NO,air}$ where Pe_1 is the Peclet number at z-position z_1, representing the ratio of the rate of bulk convection of NO to rate of axial diffusion, and α is proportional to

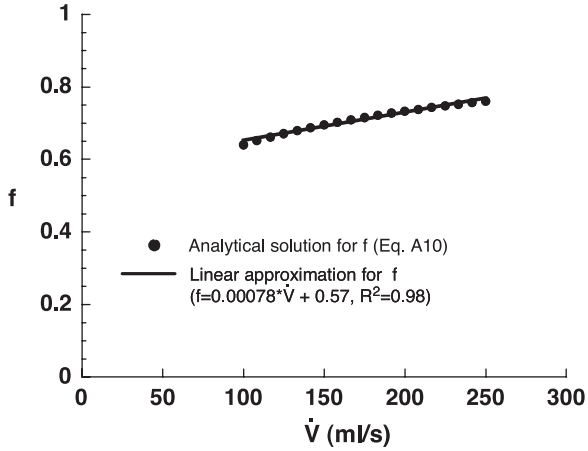

Fig. 5. Function f (*Eq. A10*, solid points) is plotted as a function of exhalation flow, $\dot{V}$ (ml/s), over the flow range of 100–250 ml/s. The solid line represents the linear fit of the 19 data points ($f = 0.00078*\dot{V}+0.57$, $r^2 = 0.98$). The function f is a monotonically increasing function of $\dot{V}$ and is >0.95 for $\dot{V}$ > 2.5 l/s.

the ratio of the rate of radial diffusion of NO to rate of axial diffusion of NO. Inserting these relationships into *Eqs. A1-A3* results in the following simpler set of equations,

$$\phi'' + [\mathrm{Pe}_1 x^2 + 2x^{-1}]\phi' + \alpha = 0 \qquad (A5)$$

with boundary conditions,

$$\phi(x = 1) = 1 \qquad (A6)$$

$$\phi'(x = x_2) = 0 \qquad (A7)$$

where ϕ' and ϕ'' are the first and second derivatives with respect to x. The solution to *Eq. A5* (second-order inhomogeneous ordinary differential equation with variable coefficients) can be solved analytically for the concentration of NO exiting the mouth ($C_{E_{NO}}$, equivalent to C_{NO} at position z_2 or ϕ at position x_2) by using an integrating factor and integrating by parts. The result is,

$$\phi(x_2) = 1 + \frac{\alpha}{\mathrm{Pe}_1}\left\{\left(\frac{\mathrm{Pe}_1}{3}\right)^{1/3} e^{\frac{\mathrm{Pe}_1}{3}}\left[\Gamma\left\{\left(\frac{\mathrm{Pe}_2}{3}\right),\frac{2}{3}\right\} - \Gamma\left\{\left(\frac{\mathrm{Pe}_1}{3}\right),\frac{2}{3}\right\}\right] - x_2^{-1}\right. \qquad (A8)$$

where Pe_2 is the Peclet number at position z_2 ($z_2\dot{V}/D_{NO,air}\,A_2$), and $\Gamma(u,n)$ is the lower incomplete gamma function defined by,

$$\Gamma(u,n) = \int_0^u t^{n-1}e^{-1}dt \qquad (A9)$$

One can rewrite *Eq. A8* by reintroducing the dimensional parameters to arrive at *Eq. 2* in the main body of the text where,

$$f = \left\{\frac{\left(\frac{\mathrm{Pe}_1}{3}\right)^{1/3} e^{\frac{\mathrm{Pe}_1}{3}}\left[1.354 - \Gamma\left(\frac{\mathrm{Pe}_1}{3},\frac{2}{3}\right)\right] - x_2^{-1}}{1 - x_2^{-1}}\right\} \qquad (A10)$$

In *Eq. A10*, $\Gamma(\mathrm{Pe}_2,2/3)$ has been replaced by the constant value of 1.354, which is valid for exhalation flows >10 μl/s. Figure 5 shows the dependence of f with exhalation flow over the flow range $100<\dot{V}<250$ ml/s. Note the near linear relationship in which f can be approximated ($r^2 = 0.98$) by the much simpler form,

$$f = 0.00078(\dot{V}) + 0.57 \qquad (A11)$$

which can then be inserted into *Eq. 2* as shown in the main text to arrive at *Eqs. 3–5*.

ACKNOWLEDGMENTS

We thank the General Clinical Research Center at University of California, Irvine.

GRANTS

This work was supported by grants from the National Institutes of Health (HL-070645 and RR-00827).

REFERENCES

1. **Alving K, Weitzberg E, Lundberg JM.** Increased amount of nitric oxide in exhaled air of asthmatics. *Eur Respir J* 6: 1368–1370, 1993.
2. **ATS/ERS.** Recommendations for standardized procedures for the online and offline measurement of exhaled lower respiratory nitric oxide and nasal nitric oxide, 2005. *Am J Respir Crit Care Med* 171: 912–930, 2005.
3. **Barnes PJ, Kharitonov SA.** Exhaled nitric oxide: a new lung function test. *Thorax* 51: 233–237, 1996.
4. **Berkman N, Avital A, Breuer R, Bardach E, Springer C, Godfrey S.** Exhaled nitric oxide in the diagnosis of asthma: comparison with bronchial provocation tests. *Thorax* 60: 383–388, 2005.
5. **Bouhuys A.** Respiratory dead space. In: *Handbook of Physiology. The Respiratory System. Gas Exchange*. Bethesda, MD: Am Physiol Soc., 1987, p. 699–714.
6. **Condorelli P, Shin HW, George SC.** Characterizing airway and alveolar nitric oxide exchange during tidal breathing using a three-compartment model. *J Appl Physiol* 96: 1832–1842, 2004.
7. **Dupont LJ, Demedts MG, Verleden GM.** Prospective evaluation of the validity of exhaled nitric oxide for the diagnosis of asthma. *Chest* 123: 751–756, 2003.
8. **Gelb AF, Taylor CF, Nussbaum E, Gutierrez C, Schein A, Shinar CM, Schein MJ, Epstein JD, Zamel N.** Alveolar and airway sites of nitric oxide inflammation in treated asthmatics. *Am J Respir Crit Care Med* 170: 737–741, 2004.
9. **George SC, Hogman M, Permutt S, Silkoff PE.** Modeling pulmonary nitric oxide exchange. *J Appl Physiol* 96: 831–839, 2004.
10. **Girgis RE, Gugnani MK, Abrams J, Mayes MD.** Partitioning of alveolar and conducting airway nitric oxide in scleroderma lung disease. *Am J Respir Crit Care Med* 165: 1587–1591, 2002.
11. **Gustafsson LE, Leone AM, Persson MG, Wiklund NP, Moncada S.** Endogenous nitric oxide is present in the exhaled air of rabbits, guinea pigs and humans. *Biochem Biophys Res Commun* 181: 852–857, 1991.
12. **Hanna LM, Scherer PW.** Measurement of local mass transport coefficients in a cast model of the human upper respiratory tract. *J Biomech Eng* 108: 12–18, 1986.
13. **Hogman M, Drca N, Ehrstedt C, Merilainen P.** Exhaled nitric oxide partitioned into alveolar, lower airways and nasal contributions. *Respir Med* 94: 985–991, 2000.
14. **Hogman M, Holmkvist T, Wegener T, Emtner M, Andersson M, Hedenstrom H, Merilainen P.** Extended NO analysis applied to patients with COPD, allergic asthma and allergic rhinitis. *Respir Med* 96: 24–30, 2002.
15. **Hogman M, Stromberg S, Schedin U, Frostell C, Hedenstierna G, Gustaffson LE.** Nitric oxide from the human respiratory tract efficiently quantified by standardised single breath measurements. *Acta Physiol Scand* 159: 345–346, 1997.
16. **Lehtimäki L, Kankaanranta H, Saarelainen S, Hahtola P, Järvenpää R, Koivula T, Turjanmaa V, Moilanen E.** Extended exhaled NO measurement differentiates between alveolar and bronchial inflammation. *Am J Respir Crit Care Med* 163: 1557–1561, 2001.
17. **Lehtimaki L, Turjanmaa V, Kankaanranta H, Saarelainen S, Hahtola P, Moilanen E.** Increased bronchial nitric oxide production in patients with asthma measured with a novel method of different exhalation flow rates. *Ann Med* 32: 417–423, 2000.
18. **Pietropaoli AP, Perillo IB, Torres A, Perkins PT, Frasier LM, Utell MJ, Frampton MW, Hyde RW.** Simultaneous measurement of nitric oxide production by conducting and alveolar airways of humans. *J Appl Physiol* 87: 1532–1542, 1999.
19. **Pijnenburg MW, Hofhuis W, Hop WC, De Jongste JC.** Exhaled nitric oxide predicts asthma relapse in children with clinical asthma remission. *Thorax* 60: 215–218, 2005.
20. **Rottier BL, Cohen J, van der Mark TW, Douma WR, Duiverman EJ, and ten Hacken NH.** A different analysis applied to a mathematical model on output of exhaled nitric oxide. *J Appl Physiol* 99: 378–380, 2005.
21. **Shin HW, Condorelli P, George SC.** Examining axial diffusion of nitric oxide in the lungs using heliox and breath hold. *J Appl Physiol* 100: 623–630, 2006.
22. **Shin HW, Condorelli P, George SC.** A new and more accurate technique to characterize airway nitric oxide using different breath-hold times. *J Appl Physiol* 98: 1869–1877, 2005.
23. **Shin HW, Condorelli P, Rose-Gottron CM, Cooper DM, George SC.** Probing the impact of axial diffusion on nitric oxide exchange dynamics with heliox. *J Appl Physiol* 97: 874–882, 2004.
24. **Shin HW, George SC.** Impact of axial diffusion on nitric oxide exchange in the lungs. *J Appl Physiol* 93: 2070–2080, 2002.
25. **Shin HW, Rose-Gottron CM, Cooper DM, Hill MA, George SC.** Impact of high intensity exercise on flow-independent NO exchange parameters. *Med Sci Sports Exerc* 35: 995–1003, 2003.
26. **Shin HW, Rose-Gottron CM, Cooper DM, Newcomb RL, George SC.** Airway diffusing capacity of nitric oxide and steroid therapy in asthma. *J Appl Physiol* 96: 65–75, 2004.

27. **Shin HW, Rose-Gottron CM, Perez F, Cooper DM, Wilson AF, George SC.** Flow-independent nitric oxide exchange parameters in healthy adults. *J Appl Physiol* 91: 2173–2181, 2001.
28. **Shin HW, Rose-Gottron CM, Sufi RS, Perez F, Cooper DM, Wilson AF, George SC.** Flow-independent nitric oxide exchange parameters in cystic fibrosis. *Am J Respir Crit Care Med* 165: 349–357, 2002.
29. **Silkoff PE, McClean PA, Slutsky AS, Furlott HG, Hoffstein E, Wakita S, Chapman KR, Szalai JP, Zamel N.** Marked flow-dependence of exhaled nitric oxide using a new technique to exclude nasal nitric oxide. *Am J Respir Crit Care Med* 155: 260–267, 1997.
30. **Silkoff PE, Sylvester JT, Zamel N, Permutt S.** Airway nitric oxide diffusion in asthma. Role in pulmonary function and bronchial responsiveness. *Am J Respir Crit Care Med* 161: 1218–1228, 2000.
31. **Smith AD, Cowan JO, Brassett KP, Herbison GP, Taylor DR.** Use of exhaled nitric oxide measurements to guide treatment in chronic asthma. *N Engl J Med* 352: 2163–2173, 2005.
32. **Tsoukias NM, George SC.** A two-compartment model of pulmonary nitric oxide exchange dynamics. *J Appl Physiol* 85: 653–666, 1998.
33. **Tsoukias NM, Shin HW, Wilson AF, George SC.** A single breath technique with variable flow rate to characterize nitric oxide exchange dynamics in the lungs. *J Appl Physiol* 91: 477–487, 2001.
34. **Tsoukias NM, Shin HW, Wilson AF, George SC.** A single-breath technique with variable flow rate to characterize nitric oxide exchange dynamics in the lungs. *J Appl Physiol* 91: 477–487, 2001.
35. **Tsoukias NM, Tannous Z, Wilson AF, George SC.** Single-exhalation profiles of NO and CO_2 in humans: effect of dynamically changing flow rate. *J Appl Physiol* 85: 642–652, 1998.
36. **Van Muylem A, Noel C, Paiva M.** Modeling of impact of gas molecular diffusion on nitric oxide expired profile. *J Appl Physiol* 94: 119–127, 2003.
37. **Weibel E.** *Morphometry of the Human Lung*. Berlin: Springer-Verlag, 1963.